JGP Journal of General Physiology

RESEARCH ARTICLE

Histidine^{168} is crucial for ΔpH-dependent gating of the human voltage-gated proton channel, hH$_V$1

Vladimir V. Cherny[1], Deri Morgan[1], Sarah Thomas[2], Susan M.E. Smith[2], and Thomas E. DeCoursey[1]

We recently identified a voltage-gated proton channel gene in the snail *Helisoma trivolvis*, HtH$_V$1, and determined its electrophysiological properties. Consistent with early studies of proton currents in snail neurons, HtH$_V$1 opens rapidly, but it unexpectedly exhibits uniquely defective sensitivity to intracellular pH (pH$_i$). The H$^+$ conductance (g_H)-*V* relationship in the voltage-gated proton channel (H$_V$1) from other species shifts 40 mV when either pH$_i$ or pH$_o$ (extracellular pH) is changed by 1 unit. This property, called ΔpH-dependent gating, is crucial to the functions of H$_V$1 in many species and in numerous human tissues. The HtH$_V$1 channel exhibits normal pH$_o$ dependence but anomalously weak pH$_i$ dependence. In this study, we show that a single point mutation in human hH$_V$1—changing His^{168} to Gln^{168}, the corresponding residue in HtH$_V$1—compromises the pH$_i$ dependence of gating in the human channel so that it recapitulates the HtH$_V$1 response. This location was previously identified as a contributor to the rapid gating kinetics of H$_V$1 in *Strongylocentrotus purpuratus*. His^{168} mutation in human H$_V$1 accelerates activation but accounts for only a fraction of the species difference. H168Q, H168S, or H168T mutants exhibit normal pH$_o$ dependence, but changing pH$_i$ shifts the g_H-*V* relationship on average by <20 mV/unit. Thus, His^{168} is critical to pH$_i$ sensing in hH$_V$1. His^{168}, located at the inner end of the pore on the S3 transmembrane helix, is the first residue identified in H$_V$1 that significantly impairs pH sensing when mutated. Because pH$_o$ dependence remains intact, the selective erosion of pH$_i$ dependence supports the idea that there are distinct internal and external pH sensors. Although His^{168} may itself be a pH$_i$ sensor, the converse mutation, Q229H, does not normalize the pH$_i$ sensitivity of the HtH$_V$1 channel. We hypothesize that the imidazole group of His^{168} interacts with nearby Phe^{165} or other parts of hH$_V$1 to transduce pH$_i$ into shifts of voltage-dependent gating.

Introduction

Voltage-gated proton channels, H$_V$1, possess several distinctive or unique properties (DeCoursey, 2015). They are exquisitely proton selective with single-channel currents in the femtoampere range (Cherny et al., 2003). Perhaps because the conduction pathway is narrow and lacks a continuous water wire (Kulleperuma et al., 2013; Morgan et al., 2013; Chamberlin et al., 2014; Dudev et al., 2015), no high-affinity blockers exist that act by simple occlusion of the pore. The most potent inhibitor is Zn^{2+}, which binds competitively with protons to two histidines in the external vestibule of human H$_V$1 (hH$_V$1) and interferes with channel opening (Cherny and DeCoursey, 1999; Takeshita et al., 2014). Although controversial (Bennett and Ramsey, 2017; DeCoursey, 2017), the conduction pathway includes an aspartate that appears to be obligatorily protonated and deprotonated during permeation (DeCoursey, 2003; Musset et al., 2011; Smith et al., 2011; Dudev et al., 2015; van Keulen et al., 2017). Consequently, H$^+$ conduction has anomalously large temperature dependence (DeCoursey and Cherny, 1998; Kuno et al., 2009) and deuterium isotope effects (DeCoursey and Cherny, 1997) when compared with other channels. H$_V$1 in many species are dimers (Koch et al., 2008; Lee et al., 2008; Tombola et al., 2008), but monomeric constructs also function with fairly subtle differences from the dimer (Koch et al., 2008; Tombola et al., 2008; Musset et al., 2010).

Perhaps the most unusual property of H$_V$1 is ΔpH-dependent gating, a unique mechanism that is essential to all its functions. Although H$_V$1 is a voltage-gated ion channel, the voltage at which all known H$_V$1 open is strongly dependent on pH. Increasing pH$_o$ or decreasing pH$_i$ shifts the H$^+$ conductance (g_H)-*V* relationship negatively by ~40 mV/unit. At symmetrical pH (pH$_o$ = pH$_i$), the threshold for activation in most species is 10–20 mV (Cherny et al., 1995; DeCoursey, 2013). The combination of these properties ensures that under almost all conditions encountered by living cells, H$_V$1 opens only when the electrochemical gradient for H$^+$ is outward, so that opening H$_V$1 channels results in

---

[1]Department of Physiology & Biophysics, Rush University, Chicago, IL; [2]Department of Molecular and Cellular Biology, Kennesaw State University, Kennesaw, GA.

Correspondence to Thomas E. DeCoursey: tdecours@rush.edu.

Rockefeller University Press

J. Gen. Physiol. 2018 Vol. 150 No. 6 851–862

https://doi.org/10.1085/jgp.201711968

```
H._trivolvis_HtHv1   E V S L K I F I E G K - H L L K Q P A E V F D A I V V I V S F T L D
L._stagnalis_LsHv1   E V S L K I F M E G T - H L L K Q P A E V F D A V V V I V S F T L D
S._purpuratus_SpHv1  E L L I K I P V F R M - E F F R S K L E V F D G I I I V I S F V L D
E._huxleyi_EhHv1     E L L T L L A A S G L R D F F S N V Y Y V L D I V I V S A S L V L E
K._veneficum_kHv1    E N M L L V L A N G C - R F F A N P F H I L D I V V V V V S V G F E
L._polyedrum_LpHv1   E Q L L L I A A M R G - A Y F R E K L M V L D G F V I T L S L L L E
H._sapiens_hHv1      E I I F K L F V F R L - E F F H H K F E I L D A V V V V V S F I L D
M._musculus_mHv1     E I F F K I F V F R L - E F F H H K F E I L D A F V V V V S F V L D
O._cuniculus_OcHv1   E I S L K I F V F R L - E F F H H K F E I L D A V V V V V S F I L D
R._rattus_RrHv1      E I S L K V F V F R L - E F F H H K F E I L D A I V V V V S F V L D
C._griseus_CgHv1     E I F F K I F V F R L - E F F H H K F E I L D A V V V V V S F V L D
```

Figure 1. **Alignment of H_V1 S2–S3 linker and nearby regions (E153–D185 in hH_V1).** H_V1 from several species were characterized as activating rapidly (green background: HtH_V1, LsH_V1, and SpH_V1) or slowly (pink background: hH_V1, mH_V1, OcH_V1, RrH_V1, and CgH_V1) based on available electrophysiological data. Unshaded species exhibit intermediate kinetics. In hH_V1 numbering, the asterisk (*) indicates the position corresponding to the throttle histidine H168; the caret (^) indicates the position corresponding to F165. The S2–S3 linker in hH_V1 encompasses K157–F165 (Li et al., 2015).

acid extrusion from cells (DeCoursey, 2003). Functions of H_V1 beyond acid extrusion, such as compensating electrically for the electrogenic activity of NADPH oxidase (Henderson et al., 1987; DeCoursey et al., 2003; DeCoursey, 2010), also require ΔpH dependent gating to enable H_V1 to open appropriately (Murphy and DeCoursey, 2006).

The phenomenon of ΔpH-dependent gating seems to be remarkably robust. Despite at least 171 different H_V1 mutants having been characterized electrophysiologically (DeCoursey et al., 2016), mutation at only one position, Trp^{207} (in hH_V1 numbering), significantly altered ΔpH-dependent gating (Cherny et al., 2015). Mutation to this Trp resulted in premature saturation of the response to pH_o but did not affect pH_i responses. Recently identified H_V1 in a few species (Cherny et al., 2015; Chaves et al., 2016), including the voltage-gated proton channel gene in the snail *Helisoma trivolvis* (HtH_V1; Thomas et al., in this issue), have an exaggerated pH_o response, shifting more than 40 mV/unit. Evaluation of three dozen hH_V1 mutants revealed shifts of the absolute voltage dependence over a 270-mV range, but every mutant still exhibited an ~40-mV/pH unit shift from whatever its starting voltage was (Ramsey et al., 2010). We were therefore surprised to find that despite a robust pH_o response, the WT HtH_V1 channel has anomalously weak pH_i dependence, with the g_H-V relationship shifting just 20 mV/unit or less (Thomas et al., 2018). While testing several possible explanations for the rapid gating of snail HtH_V1, we serendipitously discovered that replacement of a single amino acid, His^{168}, in the human channel nearly abolishes its pH_i dependence. We conclude that His^{168} is a crucial component of pH_i sensing in hH_V1.

Materials and methods

Electrophysiological and mutagenesis methods for HtH_V1 are described in the accompanying article (Thomas et al., 2018); mutagenesis of hH_V1 was described previously (Musset et al., 2010). A triple mutant of hH_V1 (H167N/H168V/K168N) was supplied by I. Scott Ramsey and David E. Clapham (Harvard Medical School, Boston, MA). Statistical comparison of groups was done by using Student's *t* test.

Sequence analysis

46 full-length H_V1 sequences, including 11 electrophysiologically confirmed and 13 high-confidence sequences from protists—previously shown to be more diverse than animal H_V1 (Smith et al., 2011)—were aligned with MAFFT (Katoh and Standley, 2013). Sequences were trimmed to the voltage-sensing domain as described previously (Smith et al., 2011). Sequences that were not confirmed electrophysiologically were excluded, and empty

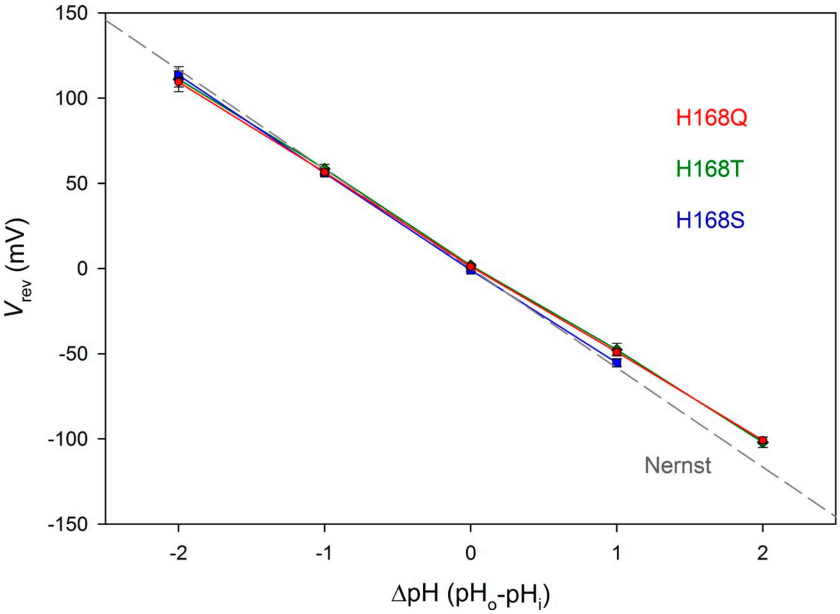

Figure 2. **His^{168} mutants are proton selective.** Mean ± SEM values for the reversal potential (V_{rev}) are plotted for 12 H168Q, 9 H168T, and 6 H168S cells or patches. The linear regression slope for each mutant is −52.6, −53.2, and −56.3 mV/unit change in ΔpH, respectively. For comparison, the gray dashed line shows the Nernst potential, E_H, expected for perfect H^+ selectivity.

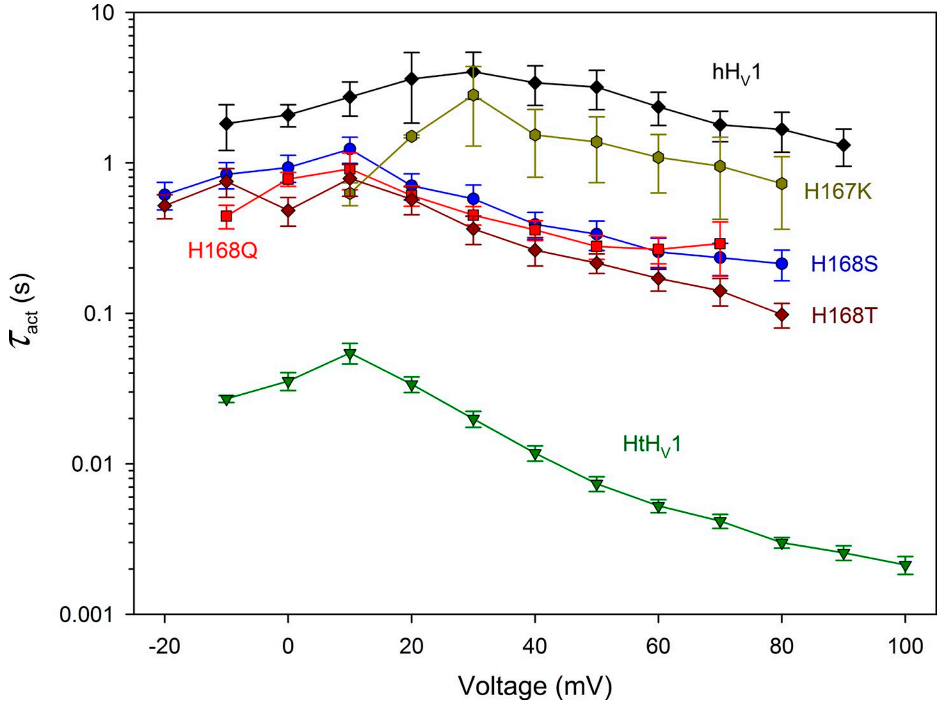

Figure 3. **The throttle histidine explains only a fraction of the rapid activation of HtH$_V$1.** Activation time constants (τ_{act}) were determined by single exponential fits to currents in WT HtH$_V$1, WT hH$_V$1, and in four hH$_V$1 mutants, as indicated, all at pH$_o$ 7 and pH$_i$ 7. Mean ± SEM is plotted for 3–12 WT hH$_V$1, 2–3 H167K, 3–6 H168S, 3–9 H168Q, 3–6 H168T, and 7–17 WT HtH$_V$1. At all voltages from −10 to +80 mV, the WT hH$_V$1 value is significantly larger than that of H168T, H168S, and H168Q combined and larger than HtH$_V$1 ($P < 0.01$). The WT hH$_V$1 data were taken from Cherny et al. (2015) and the HtH$_V$1 data from Thomas et al. (2018).

columns removed from the alignment. The activation (opening) kinetics of electrophysiologically confirmed sequences were characterized as fast (*H. trivolvis*, HtH$_V$1; *Lymnaea stagnalis*, LsH$_V$1; and *Strongylocentrotus purpuratus*, SpH$_V$1) or slow (*Homo sapiens,* hH$_V$1; *Mus musculus*, mH$_V$1; *Oryctolagus cuniculus*, OcH$_V$1; *Rattus norvegicus*, RnH$_V$1; and *Cricetulus griseus*, CgH$_V$1); sequences with intermediate or unknown kinetics were removed. To identify sequence sites that distinguish sequence subfamilies, the alignment was submitted to the SPEER server (Chakraborty et al., 2012) with either user-defined (two subfamilies) or automated subgrouping and the following parameters: single-submission eight sequences, Relative Entropy term, PC Property Distance term, and Type. The same alignment but in randomized sequence order was also submitted with the automated subgrouping parameter and all other parameters as above. Sites corresponding to His^{167} and His^{168} in hH$_V$1 were identified as appearing in the top 10 sites identified in all analyses and having a P value of <0.05 in at least one analysis.

Results

Is His^{168} responsible for the slow gating kinetics of hH$_V$1?

In our companion article (Thomas et al., 2018), we reported the identification of an H$_V$1 in a snail *H. trivolvis* (HtH$_V$1) that exhibited rapid activation kinetics as reported for native proton currents in other snails (Byerly et al., 1984). We performed an analysis of subfamily determining sites to distinguish H$_V$1 sequences with fast versus slow gating kinetics. Species categorized as having fast gating included snails, HtH$_V$1 (Thomas et al., 2018) and *L. stagnalis*, LsH$_V$1 (Byerly et al., 1984); and sea urchin, *S. purpuratus*, SpH$_V$1 (Sakata et al., 2016) and are shaded green in Fig. 1. Species with slow gating are human, hH$_V$1 (Bernheim et al., 1993; DeCoursey and Cherny, 1993; Demaurex et al., 1993); mouse, mH$_V$1 (Kapus et al., 1993); rabbit, *O. cuniculus*, OcH$_V$1 (Nordström et al., 1995); rat, *R. norvegicus*, RnH$_V$1 (DeCoursey, 1991); and Chinese hamster, *C. griseus*, CgH$_V$1 (Cherny et al., 1997) and are shaded pink in Fig. 1. This analysis pointed to two residues corresponding to His^{167} and His^{168} in hH$_V$1 numbering; these residues are in the intracellular S2/S3 loop, extending into the S3 transmembrane helix. Sakata et al. (2016) found that substituting either Ser or Thr for His^{164} in mH$_V$1, which corresponds to His^{168} in hH$_V$1 (Fig. 1, asterisk), accelerated activation kinetics by an order of magnitude, raising the possibility that His in this position governs activation kinetics, acting as a "throttle." The same substitutions at the neighboring His^{163} had no effect. For these reasons we focused our experiments on the S2/S3 loop area.

Similar to Sakata et al. (2016), we engineered mutations of His^{168}, replacing it with Ser (H168S) or Thr (H168T). Because activation of snail HtH$_V$1 is distinctly faster than that of sea urchin SpH$_V$1, we reasoned that replacing His^{168} with Gln, which is at the corresponding position in HtH$_V$1 (H168Q), should cause even faster kinetics. As a control, we replaced the neighboring His^{167} in hH$_V$1 with Lys (H167K), which occupies this position in HtH$_V$1 (Fig. 1). Finally, we tested a triple mutant, in which three consecutive titratable amino acids (His^{168} and its immediate neighbors) were all replaced by neutral residues (H167N/H168V/K169N). Robust proton selective currents were observed in all mutants. Results from H168S, H168T, and H168Q mutants

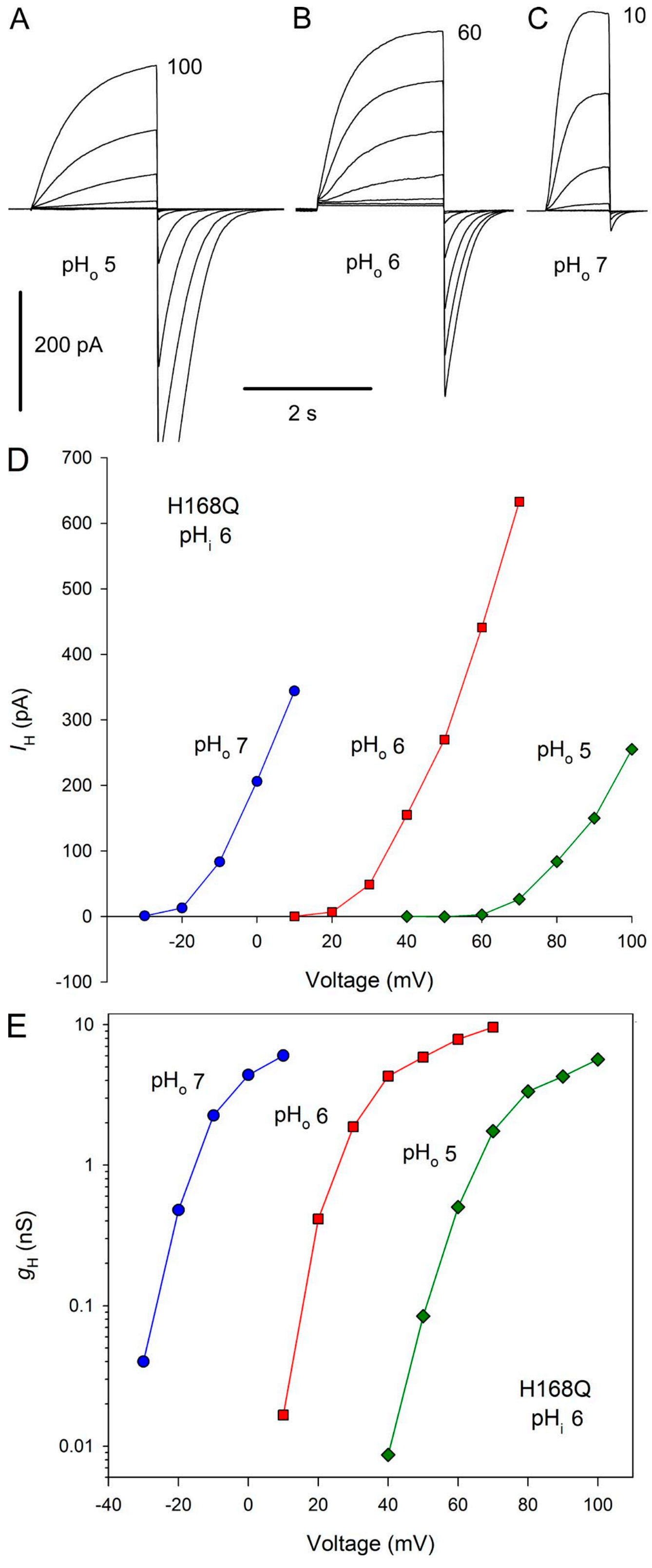

Figure 4. **Gating of His^{168} mutants has normal pH$_o$ dependence. (A–C)** Families of currents in a cell expressing H168Q with pH$_i$ 6 and pH$_o$ 5, 6, and 7, with pulses in 10-mV increments up to the voltage indicated. Holding potential, V_{hold} was −40 mV (A and B) or −60 mV (C). **(D and E)** Proton current–voltage curves (D) and g_H-V relationships (E) from the families in A–C exhibit a normal 40-mV shift/unit change in pH$_o$.

were indistinguishable, and we thus refer to all such mutants as H168X. Fig. 2 shows that the reversal potential (V_{rev}) in the three H168X mutants was close to the Nernst potential, confirming proton selectivity.

Fig. 3 illustrates the effects of these mutations on channel-opening kinetics. Replacing His^{168} with any of the three amino acids (Ser, Thr, or Gln) produced a 10-fold speeding of the activation (opening) time constant (τ_{act}) in the positive voltage range, much like the analogous effect in mH$_V$1 (Sakata et al., 2016). Mutating the neighboring His^{167} had no clear effect. That the effects of the three substituents (Ser, Thr, or Gln) were identical suggests that the speeding of activation is caused by removing the imidazole group of His and is not caused by introducing other side chains at this position. Thus, the hydroxyl group of Thr or Ser was no more or less effective than the amide group of Gln. Presumably, His^{168} interacts specifically with other parts of the hH$_V$1 channel in a manner that results in slower activation. Nevertheless, despite the distinct acceleration caused by His^{168} removal, τ_{act} remained much slower than in the WT snail channel HtH$_V$1.

His^{168} mutation alters ΔpH-dependent gating of hH$_V$1

The His^{168} mutants exhibited normal responses to changes in pH$_o$. Families of currents in a cell expressing the H168Q mutant are shown in Fig. 4, A–C. The currents appear qualitatively like WT hH$_V$1 currents, although with somewhat faster activation. Changing pH$_o$ from 5 to 6 to 7 shifted the H$^+$ current (I_H)-V (Fig. 4 D) and g_H-V relationships (Fig. 4 E) by ~40 mV/unit. This behavior conforms to the classical "rule of forty" observed for H$_V$1 in all species thus far examined (DeCoursey, 2013), except for HtH$_V$1 as described in the companion article (Thomas et al., 2018).

In contrast, mutation of His^{168} to Ser, Thr, or Gln greatly weakened the sensitivity of the mutant channels to pH$_i$. Fig. 5, A–E shows currents in an inside-out patch with H168T at pH$_o$ 7 and pH$_i$ ranging from 5 to 9. Although the I_H-V relationship does shift positively at higher pH$_i$ (Fig. 5 F), the shift is distinctly <40 mV, especially at high pH$_i$, with the result that there are inward currents over a wide voltage range. Inward currents in WT hH$_V$1 are rarely observed and occur mainly with large outward pH gradients (Musset et al., 2008). It is evident from the g_H-V relationships (Fig. 5 G) that the shifts are ≤20 mV/unit over the entire pH$_i$ range studied.

Measurements of the position of the g_H-V relationship in several cells and patches are summarized in Fig. 6 A, quantified as $V(g_{H,max}/10)$, the voltage at which g_H reached 10% of $g_{H,max}$, its maximal value. Changes in pH$_o$ for the H168X mutants (Fig. 6 A, blue circles) produce a slope of 40 mV/unit up to pH$_o$ 8 (ΔpH = 1). This behavior is identical to the WT hH$_V$1 response (Cherny et al., 2015). Data from inside-out patches (Fig. 6 A, dark red diamonds) reveal that the H168X mutants exhibit a greatly attenuated pH$_i$ response. The entire curve has a mean slope of only 16.1 mV/unit. However, the relationship appears steeper at high ΔpH. Omitting the point at ΔpH = 2 (pH$_o$ 7, pH$_i$ 5), the mean slope drops to 12.6 mV/unit.

The behavior of the H168X mutants strikingly resembles that of WT HtH$_V$1, as illustrated in Fig. 6 B. The data for HtH$_V$1 from the companion article (Thomas et al., 2018) are replotted here (Fig. 6 B, open symbols and dotted lines) for comparison.

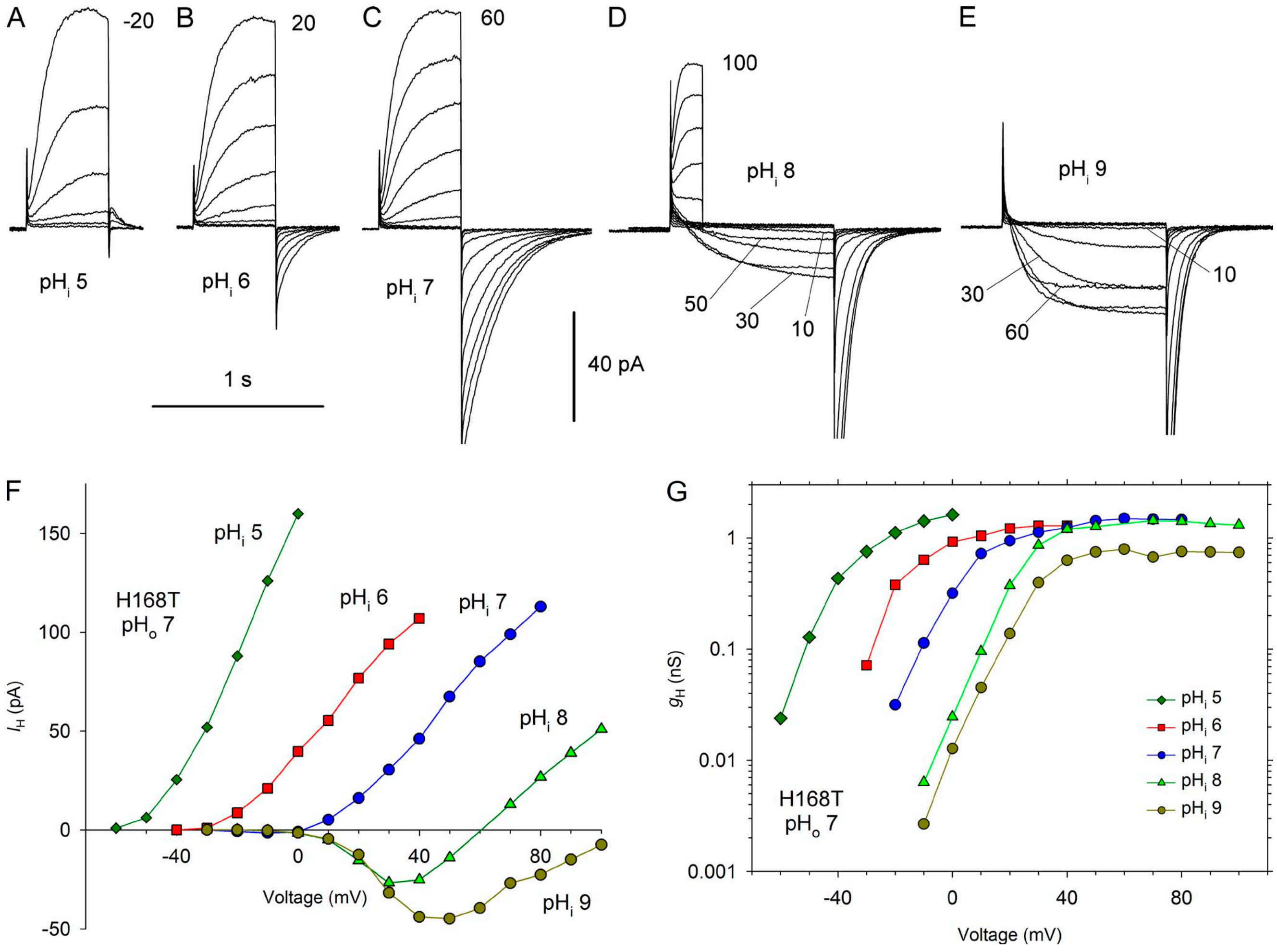

Figure 5. **Mutation of His^{168} in hH$_V$1 weakens the pH$_i$ dependence of gating. (A–E)** Families of currents at several pH$_i$ values in an inside-out patch from a cell transfected with H168T, with pH$_o$ 7 in the pipette. Pulses were applied in 10-mV increments up to the voltage indicated from V_{hold} = −80 mV (A), −60 mV (B), or −40 mV (C–E). (D) Shorter pulses were applied to 60 mV and above, and the tail currents have been removed. (E) Pulses above 60 mV were omitted for clarity. **(F)** Current–voltage curves. **(G)** g_H-V relationships from this experiment.

Comparison of pH$_o$ responses reveals that HtH$_V$1 has an exceptionally steep ΔpH dependence at pH$_o$ 7 or less, roughly 60 mV/unit. The response to pH$_o$ for H168X mutants (Fig. 6 B, shaded blue circles) is a 40-mV/unit shift, which is normal for human hH$_V$1 (Cherny et al., 2015). The response of H168X mutants to pH$_i$ changes (Fig. 6 B, red diamonds) is notably weak and closely parallels the response of WT snail HtH$_V$1. With respect to ΔpH-dependent gating, the mutation of a single amino acid, His^{168}, effectively converts the human channel into a snail channel.

The immediate neighbors of His^{168} do not appear to contribute

Located next the His^{168} that plays a critical role in pH$_i$ sensing is another His, His^{167}. We wondered whether this nearby position might share the effect. However, the single mutation H167K did not impair pH$_i$ sensing. This specific replacement was selected because HtH$_V$1 has Lys at the corresponding position (Fig. 1). Fig. 7 illustrates H$^+$ currents in an inside-out patch expressing the H167K mutant at pH$_i$ 6, 7, and 8. The g_H-V relationship shifted normally (Fig. 7 E). Mean data from three patches with H167K are plotted in Fig. 8, which shows that the pH$_i$ response of this mutant is indistinguishable from that of WT hH$_V$1. Furthermore, Fig. 3 showed that the H167K mutation did not alter activation kinetics. Evidently, His^{168} but not His^{167} is located precisely where it can strongly influence gating in response to pH$_i$.

We also tested a triple mutant, in which three consecutive titratable amino acids at the inner end of the S3 helix were replaced by neutral residues (H167N/H168V/K169N). In inside-out patches with pH$_o$ 7.5, studied at pH$_i$ 5.5, 6.5, 7.5, and 8.5, the sensitivity to pH$_i$ was weak, like that of the H168X single mutants. The mean slope by linear regression of the relationship between ΔpH and $V(g_{H,max}/10)$ in seven patches was 20.1 mV/unit, similar to 16.1 mV/unit in H168X (Fig. 6), suggesting that the amino acids neighboring His^{168} were inactive. This triple mutant was examined previously, and normal ΔpH dependence was reported (Ramsey et al., 2010). However, in that study only pH$_o$ was varied, not pH$_i$. The triple mutant, like all single His^{168} mutants, exhibits normal pH$_o$ dependence but abnormally weak pH$_i$ dependence.

Possible interaction between H168 and F165

Data on pH$_i$ sensitivity are somewhat less abundant than for pH$_o$ sensitivity, and much is derived from native tissues. Species with H$_V$1 that have been shown to exhibit classical rule of forty

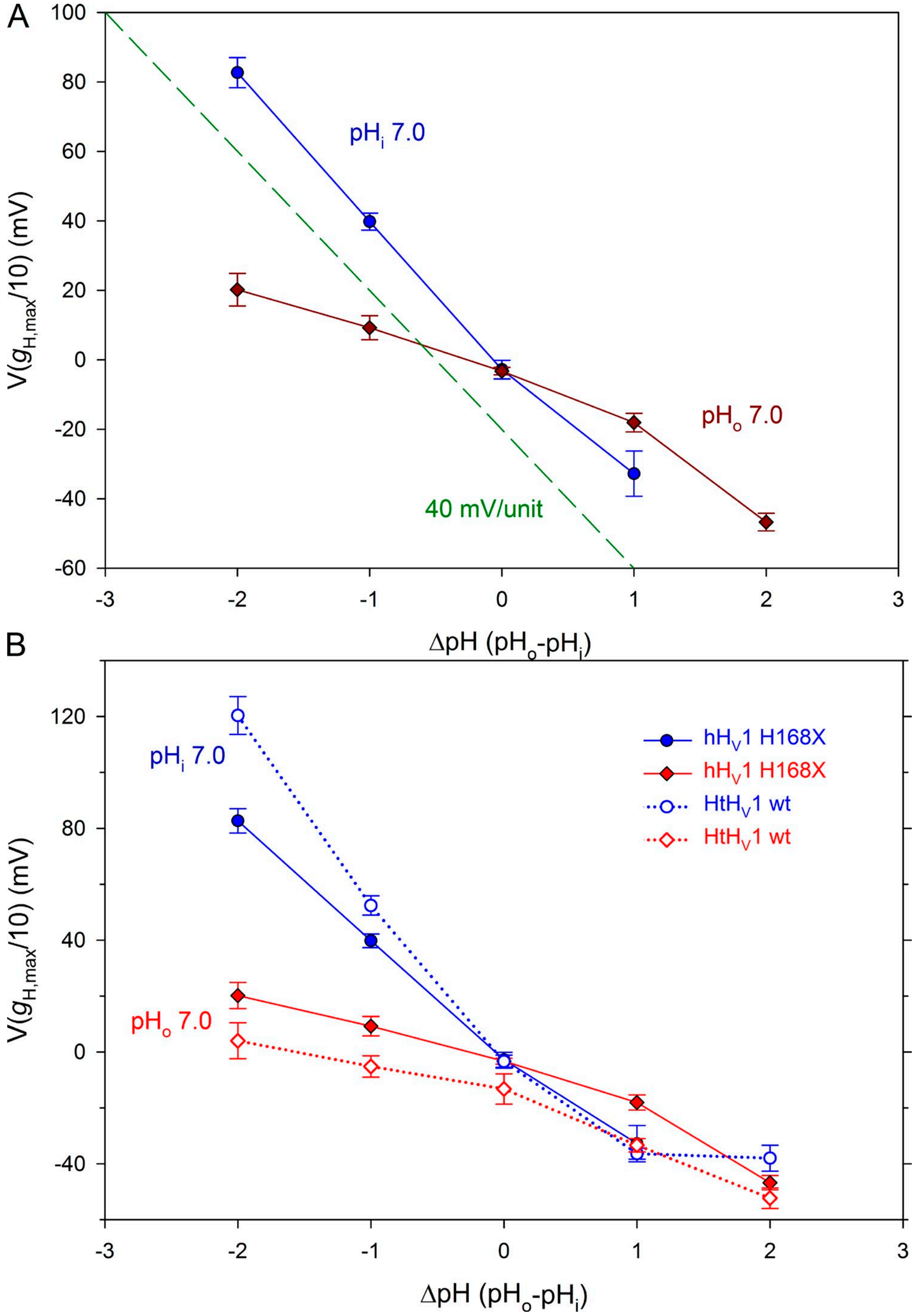

Figure 6. **The His^{168} mutation recapitulates the anomalous ΔpH dependence of HtH$_V$1. (A)** The effect of pH$_o$ and pH$_i$ on the position of the g_H-V relationship in the three H168x mutants combined (mean ± SEM) is plotted. The position of the g_H-V relationship was defined in terms of $V(g_{H,max}/10)$. The dashed green line shows a slope of 40 mV/unit for reference. The dependence of these mutants on pH$_o$ is normal, whereas their pH$_i$ response is greatly attenuated. Linear regression on all points (ignoring the obvious nonlinearity) gives a slope of 38.9 mV/unit change in pH$_o$ and 16.1 mV/unit change in pH$_i$. **(B)** The same data are replotted (shaded symbols) along with the analogous measurements for HtH$_V$1 (open symbols) taken from Fig. 9 of the companion article (Thomas et al., 2018). In whole-cell measurements, pH$_o$ was varied with pH$_i$ 7 (blue symbols). When pH$_i$ was varied by using inside-out patches with pH$_o$ 7, there was very little shift of the g_H-V relationship (red symbols). Numbers of cells for increasing ΔpH in H168X mutants for pH$_i$ 7 are 3, 10, 11, and 5 and for pH$_o$ 7 are 6, 10, 14, 11, and 4.

behavior for changes in pH$_i$ include human (Demaurex et al., 1993; Gordienko et al., 1996; Schrenzel et al., 1996; Schilling et al., 2002), mouse (Kapus et al., 1993; Szteyn et al., 2012), *Rana pipiens* (Gu and Sackin, 1995), rat (Cherny et al., 1995; DeCoursey and Cherny, 1995), *Karlodinium veneficum* (Cherny et al., 2015), *Emiliania huxleyi* (Cherny et al., 2015), and *Lingulodinium polyedrum* (Rodriguez et al., 2017). The only violators of the rule thus far are the snails *H. trivolvis* (Thomas et al., 2018) and *L. stagnalis* (Byerly et al., 1984). Another intriguing exception is a short isoform of hH$_V$1 expressed in sperm that lacks the first 68 amino

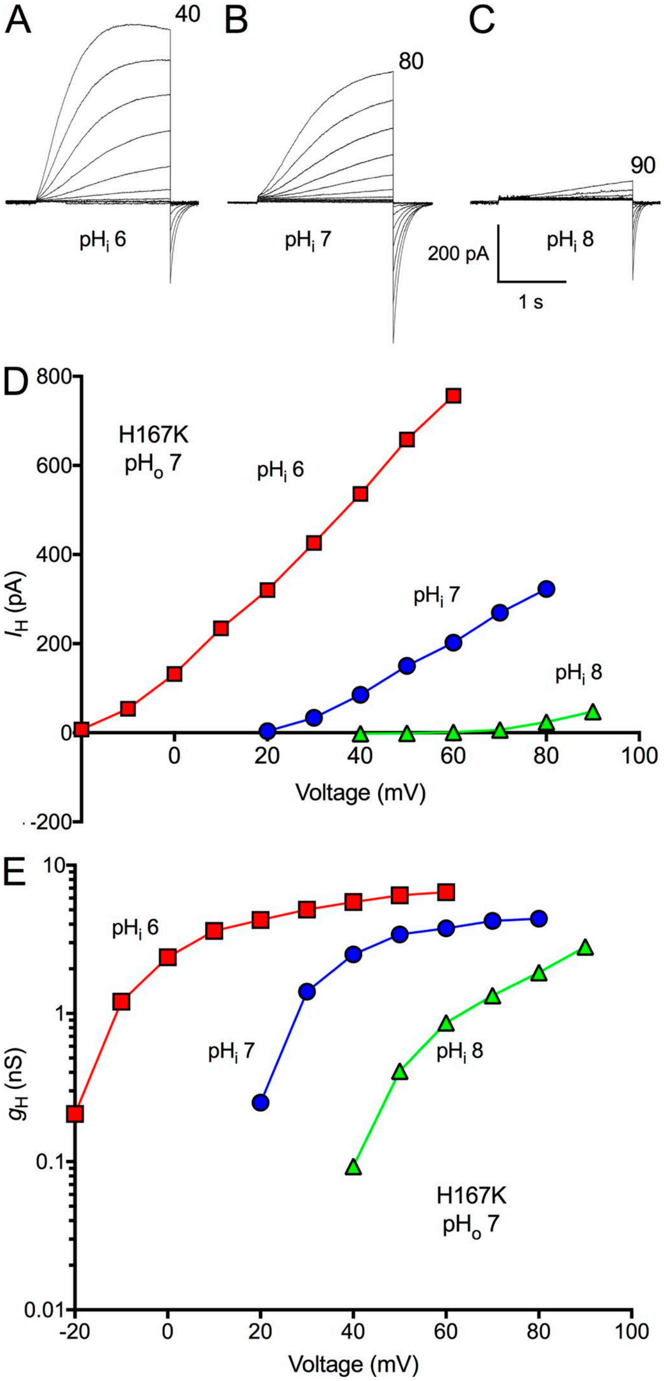

Figure 7. **The H167K mutant of hH_V1 has normal pH_i dependence. (A–C)** Families of currents are shown in an inside-out patch with pH_o 7 and pH_i 6, 7, or 8, as labeled. Pulses were applied in 10-mV increments up to the voltage indicated, from V_{hold} = −60 mV (A) or -40 mV (B and C). **(D and E)** Current–voltage curves (D) and g_H-V relationships from this patch are illustrated (E). At pH_i 8, g_H was estimated from tail current amplitudes and scaled according to g_H calculated from the outward current at 90 mV.

acids of the N terminus and has weakened pH_i sensing (Berger et al., 2017). Inspection of sequences (Fig. 1) for which pH_i sensitivity has been measured directly (HtH_V1, LsH_V1, EhH_V1, kH_V1, LpH_V1, hH_V1, mH_V1, and RnH_V1) shows that Leu substitutes for Phe at the Phe^{165} position (human numbering) in two species with rapid gating and attenuated pH_i responses, HtH_V1 and LsH_V1. Although in the available crystal structure of H_V1 (Takeshita et al., 2014) this area did not have sufficient electron density to be visualized, molecular models of H_V1 (Kulleperuma et al., 2013; Li et al., 2015) indicate that Phe^{165} could plausibly interact with the nearby His^{168} through π-stacking or cation-π interactions.

To test the idea that His^{168} interacts with Phe^{165}, we individually mutated Phe^{165} and as a control, Phe^{166}. F166L produced robust currents, and as shown in Fig. 8, pH_i sensing of F166L was essentially normal and similar to that of WT hH_V1. F165H and F165A (Fig. 8, F165X) produced currents that activated in a more negative voltage range than WT. To enable comparison of the slopes, 13.8 mV has been added to these data, so they superimpose on WT at $\Delta pH = 1$. The pH_i sensitivity of F165A and F165H was closer to WT than to that of the H168X mutants. Finally, the double mutant F165L/H168Q was also close to the single H168X mutant data (unpublished data). Although these results do not rule out the possibility of interaction between His^{168} and Phe^{165}, it appears that His^{168} is distinctly more critical for pH_i sensing.

The converse mutation Q229H fails to impart human characteristics to the *H. trivolvis* channel

The single point mutation H168X (X = T, S, Q) profoundly alters the gating and pH sensing of the human channel hH_V1, accelerating activation 10-fold and greatly attenuating the pH_i response. We next considered whether the converse mutation (Q229H) would impart humanoid characteristics to HtH_V1. In short, this mutation had no discernable effect on the gating kinetics or pH sensitivity of HtH_V1 (Fig. 9). The Q229H mutation did not slow activation; at +40 mV at pH_o 7, τ_{act} was 11.8 ± 1.4 ms (n = 17) in WT HtH_V1 (Fig. 3) and 10.0 ± 2.0 ms (n = 8) in Q229H (P = 0.53). We assessed pH_o sensitivity in whole-cell experiments. Like WT HtH_V1, activation kinetics was extremely sensitive to pH_o, whereas the deactivation or tail current (closing) time constant appeared to be pH_o independent. Like WT, changes in pH_o produced supernormal shifts in the position of the g_H-V relationship, averaging 57 mV/unit between pH_o 5 and 7 (Fig. 10), paralleling the WT response although the absolute voltages appear somewhat more negative. Similarly, the Q229H mutation did not discernibly change the weak response of HtH_V1 to changes in pH_i (Figs. 9 E and 10). In three inside-out patches studied at pH_i 5, 6, 7, and 8, the slope of the mean dependence of $V(g_{H,max}/10)$ on ΔpH was 18 mV/unit by linear regression. It is clear that the extraordinary changes to the pH_i response of the human channel resulting from His^{168} mutation reflect interactions that are not confined to this single amino acid and therefore are not easily transferred.

Discussion

Is the human hH_V1 channel slow because of the throttle residue, His^{168}?

The sea urchin proton channel, SpH_V1, exhibits rapid activation kinetics 20–60 times faster than the mouse mH_V1. Sakata et al. (2016) investigated the structural basis for this property and, by creating progressively smaller chimerae with mH_V1, finally identified a single amino acid (Ser) at the inner end of the S3 transmembrane segment that appeared largely responsible. Introducing Ser into mH_V1 (H164S) accelerated mouse activation kinetics

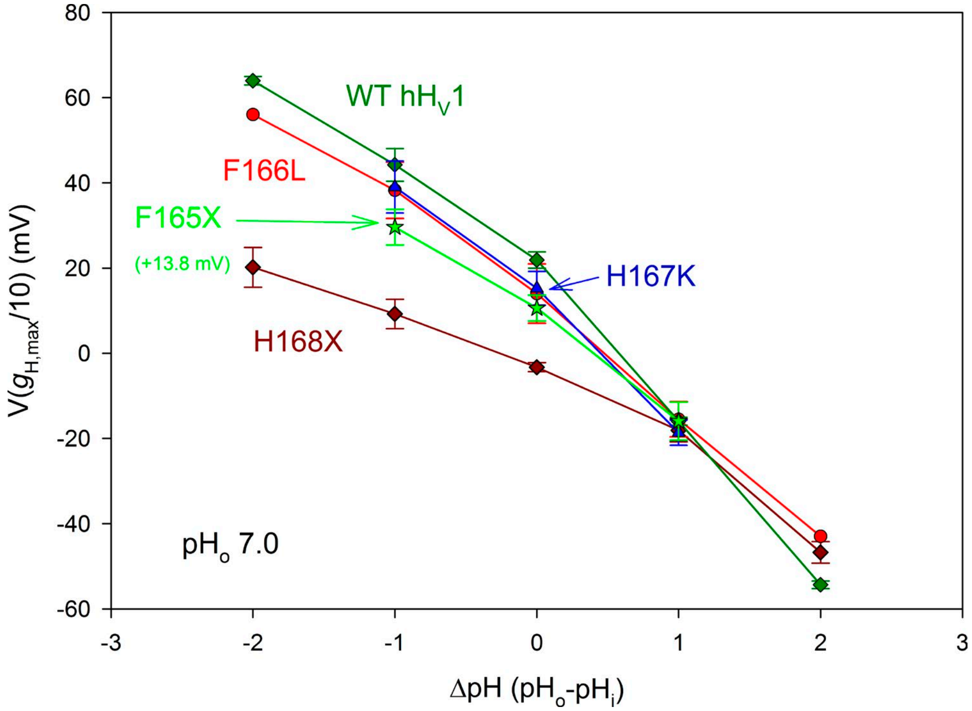

Figure 8. **The F166L and H167K mutations do not impair pH_i sensing of hH_V1.** The pH_i responses of the H168X mutants are replotted from Fig. 6. The pH_i responses of WT hH_V1, the F166L mutant of hH_V1, and the H167K mutant of hH_V1 are indistinguishable from each other. The F165X data are from three F165A and three F165H patches combined, and 13.8 mV has been added to all values to facilitate comparison with WT. All data (mean ± SEM) come from inside-out patches studied at pH_o 7, with n = 2–9 (H168X), 1–4 (F166L), 3 (H167K), and 6 (F165X).

by more than an order of magnitude. In mH_V1, H164T produced speeding similar to H164S, suggesting that the hydroxyl group is important (Sakata et al., 2016). Intriguingly, however, the converse mutation, and even substituting the entire S3 helix from mH_V1 into SpH_V1, failed to slow the kinetics of the latter.

We engineered mutations of human hH_V1 at His^{168} (the position that corresponds to His^{164} in mH_V1), replacing the His with Ser (H168S), Thr (H168T), or Gln (H168Q). In most respects, the results resembled those in mH_V1: mutations at His^{168} accelerated activation by about one order of magnitude (Fig. 3). Because HtH_V1 has Gln at the corresponding position and HtH_V1 is distinctly faster than SpH_V1, we expected that Gln substitution might produce faster activation; however, activation kinetics of H168Q were very similar to those of H168S and H168T, all of which remained much slower than that of WT HtH_V1 (Fig. 3). Because the three mutants behaved indistinguishably, we conclude that the effects result from the removal of the imidazole side chain of His^{168} and not from the side chains that replace it.

The precise location of His^{168} is important. The His immediately adjacent to His^{168} does not share its impact on gating kinetics. Sakata et al. (2016) replaced His^{163} in mH_V1 with the SpH_V1 residue at the corresponding position (H163R); this mutation had little effect on kinetics of mH_V1. We replaced His^{167} in hH_V1 with Lys, which occupies the corresponding position in HtH_V1. In neither species was activation kinetics appreciably affected (Fig. 3).

Also, similar to the results in mH_V1, the converse mutation substituting the hH_V1 residue for the HtH_V1 throttle residue, Q229H, did not slow HtH_V1 kinetics. Therefore, the mechanism by which His^{168} retards activation must require interaction with other parts of the protein that are absent in H_V1 from species with rapid gating.

His^{168} in hH_V1 is crucial for pH_i sensing

In searching for a mechanistic explanation for the rapid gating kinetics of HtH_V1, we serendipitously identified a histidine near the inner end of the channel that is crucial for pH_i sensing. Transferring the Gln^{229} from the snail channel HtH_V1 to replace His^{168} in the human channel hH_V1 (Fig. 1) reproduced the impoverished pH_i sensing of HtH_V1 almost exactly (Fig. 6 B). Because three different substituents (Ser, Thr, and Gln) had indistinguishable effects (Figs. 3 and 6), it appears that a specific property of His in this position is involved. Because the converse mutation (Q229H) did not transfer human-like pH_i sensing (or activation kinetics) to HtH_V1 (Fig. 9), His^{168} must perform pH_i sensing by interacting with its immediate environment in the human channel. This conclusion is reinforced by the fact that three unicellular species that lack His at this position (kH_V1, LpH_V1, and EhH_V1; Fig. 1) exhibit normal pH_i sensitivity (Cherny et al., 2015; Rodriguez et al., 2017). Replacing the neighboring His^{167} had no effect, and mutating both His^{167} and Lys^{169} (HHK→NVN) had no effect beyond that of His^{168} alone, indicating that the specific location at position 168 is critical.

When the ΔpH dependence of H_V1 gating was discovered (Cherny et al., 1995), the simplest model that could reproduce the entire phenomenon postulated a single pH sensor with alternating access to both internal and external solutions. An expanded model with additional complexity includes distinct external and internal pH sensors. A "counter-charge" model has been suggested in which protonation disrupts charge-pair interactions,

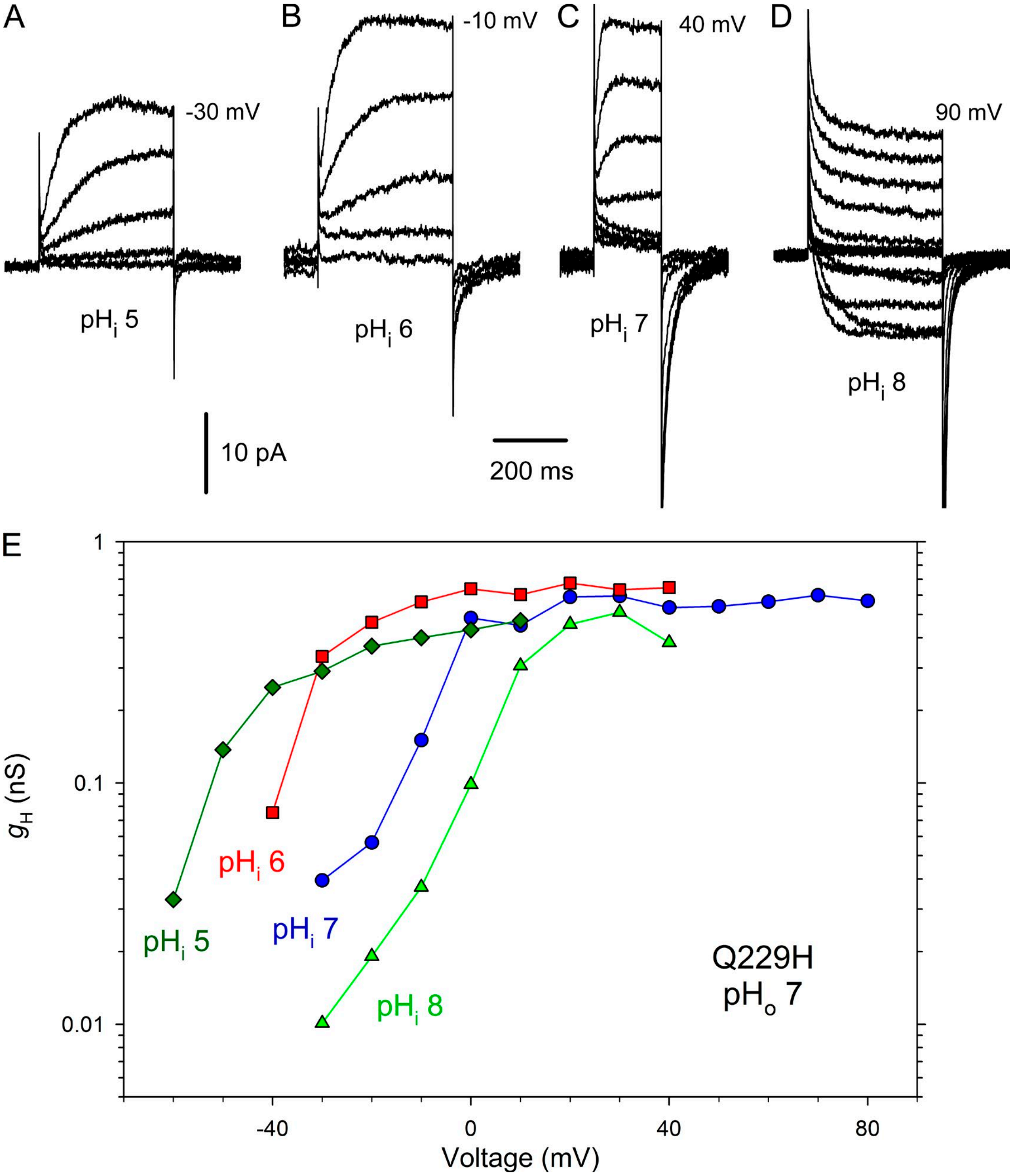

Figure 9. **The Q229H mutation does not restore human-like activation kinetics or pH$_i$ sensitivity to HtH$_V$1. (A–D)** Families of currents in an inside-out patch with pH$_o$ 7 in the pipette solution in 10-mV increments up to the voltage shown from V_{hold} = −80, −60, −40, and −40 mV, at pH$_i$ 5, 6, 7, and 8, respectively. **(E)** Currents from this patch converted to g_H produce g_H-V relationships that shift much less than 40 mV/unit. Corresponding measurements in WT HtH$_V$1 are plotted in Fig. 5 G.

so that low pH$_i$ promotes opening and low pH$_o$ promotes closing (DeCoursey, 2018). A different kind of proposal for pH sensing does not invoke titratable pH sensors; instead, protonated waters in H$_V$1 communicate information about local pH through electrostatic interactions with the voltage-sensing Arg residues in the S4 helix (Ramsey et al., 2010). Recently, the first mutation in H$_V$1 documented to compromise pH sensing was reported (Cherny et al., 2015). In these Trp mutants, pH$_o$ but not pH$_i$ sensitivity was affected, suggesting that separate pH$_o$ and pH$_i$ sensors exist in H$_V$1. Intriguingly, like the H168X mutants, these W207X mutants also dramatically accelerated hH$_V$1 gating kinetics, and HtH$_V$1 itself has extremely rapid gating.

That HtH$_V$1 has normal pH$_o$ sensitivity but anemic pH$_i$ sensitivity suggests that its ΔpH dependence is accomplished by distinct external and internal pH sensors. That the H168x mutation in hH$_V$1 selectively attenuates its pH$_i$ sensitivity without affecting its pH$_o$ sensitivity further supports the existence of distinct external and internal pH sensors.

To search for a structural basis for this species difference in pH$_i$ sensing, we compared the sequences of H$_V$1 in species in which pH$_i$ responses have been documented to obey the rule of forty (human, mouse, rat, *K. veneficum*, *E. huxleyi*, and *L. polyedrum;* excepting *R. pipiens* for which we could find no sequence), to the sequence of HtH$_V$1 with its anomalously weak

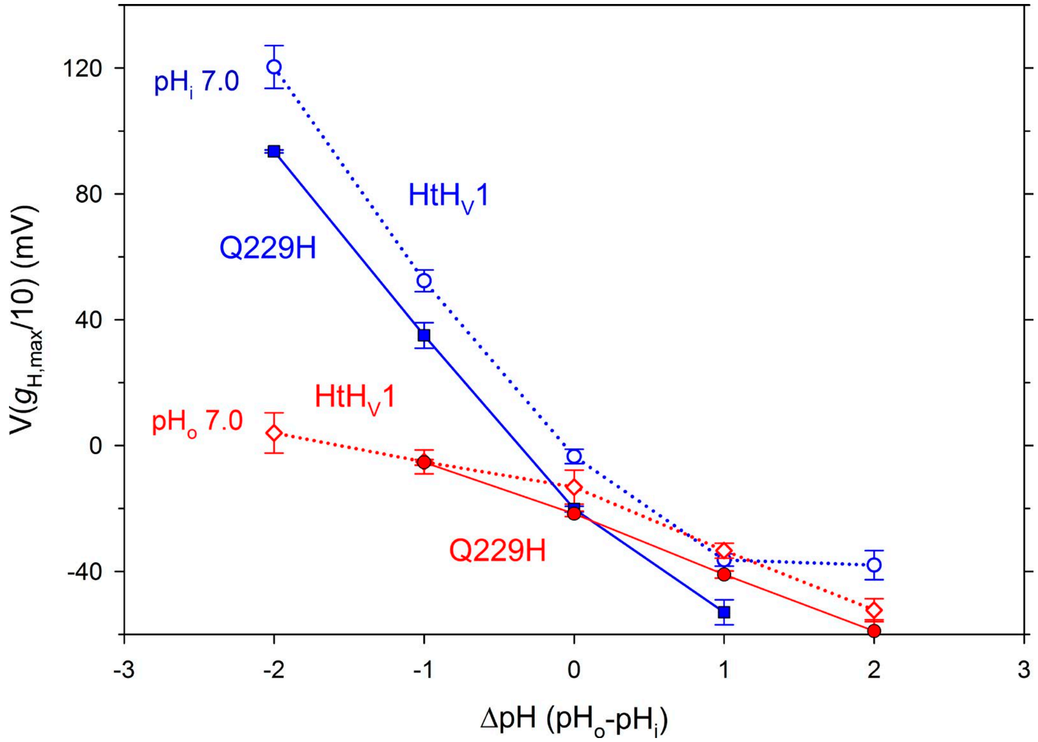

Figure 10. **The Q229H mutation does not restore human-like $\mathrm{pH_i}$ sensitivity to $\mathrm{HtH_V1}$.** The dependence of the position of the g_H-V relationship on both $\mathrm{pH_o}$ and $\mathrm{pH_i}$ is similar in WT $\mathrm{HtH_V1}$ (open symbols and dotted lines) and in the Q229H mutant (shaded symbols and solid lines). The WT data are replotted from Fig. 6 B. Mean ± SEM are shown for n = 2–5 cells with $\mathrm{pH_i}$ 7 and three inside-out patches with $\mathrm{pH_o}$ 7.

sensitivity to $\mathrm{pH_i}$. We noticed a striking substitution in $\mathrm{HtH_V1}$, in which Phe^{165} (human numbering; Fig. 1) is replaced by Leu. This position is very highly conserved: in the alignment of 46 $\mathrm{H_V1}$ sequences that includes vertebrates, invertebrates, and protists, Phe is replaced by the conservative Tyr five times, by Leu twice, and by Met once. In this context, it is important to note that the protist $\mathrm{H_V1}$ sequences are more diverse than all animal sequences (Smith et al., 2011), highlighting the very high conservation of Phe at this position. The two snail species in which Leu replaces Phe ($\mathrm{HtH_V1}$ and $\mathrm{LsH_V1}$) both have rapid gating and weak $\mathrm{pH_i}$ sensitivity (Fig. 1). In structural models of $\mathrm{H_V1}$ (Kulleperuma et al., 2013; Li et al., 2015), Phe^{165} is in a position in which it could plausibly interact with His^{168}, through π-stacking or cation-π interactions. Reasoning that such an interaction might be part of the $\mathrm{pH_i}$-sensing mechanism, we replaced Phe^{165} in $\mathrm{hH_V1}$ with Ala or His to attempt to disrupt the interaction. Both F165A and F165H exhibited $\mathrm{pH_i}$ sensing intermediate between WT and the H168x mutants but closer to WT $\mathrm{hH_V1}$. The neighboring F166L mutation did not affect $\mathrm{pH_i}$ sensing (Fig. 8). For geometrical reasons, we consider it more likely that His^{168} could interact with Phe^{165} than with Phe^{166} because the latter would be constrained by proximity. Intrahelical $i, i+2$ side-chain–side-chain contacts are statistically improbable (Walther and Argos, 1996). That Phe^{165} mutants were activated at more negative voltages than WT (Fig. 8) is consistent with F165-H168 interaction impeding $\mathrm{hH_V1}$ opening. That the insertion of His into the corresponding position in $\mathrm{HtH_V1}$ did not enhance $\mathrm{pH_i}$ sensitivity indicates that the mere presence of His at this location is not sufficient, but that to affect $\mathrm{pH_i}$ sensing requires additional interaction. Evidently, and perhaps surprisingly, the intracellular S2–S3 linker is of central importance in sensing $\mathrm{pH_i}$ in human $\mathrm{hH_V1}$. Furthermore, the selective effect of mutations in this region on $\mathrm{pH_i}$ sensing while leaving $\mathrm{pH_o}$ sensing intact supports the idea that ΔpH-dependent gating of $\mathrm{H_V1}$ relies on independent internal and external pH sensors.

Acknowledgments

This work was supported by National Institutes of Health grants GM102336 (to T.E. DeCoursey and S.M.E. Smith) and GM121462 (to T.E. DeCoursey) and National Science Foundation grant MCB-1242985 (to T.E. DeCoursey and S.M.E. Smith).

The authors declare no competing financial interests.

Author contributions: S.M.E. Smith and T.E. DeCoursey conceptualized the study. T.E. DeCoursey curated the data. S. Thomas, S.M.E. Smith, V.V. Cherny, D. Morgan, and T.E. DeCoursey performed the formal analysis. T.E. DeCoursey and S.M.E. Smith acquired the funding. V.V. Cherny and D. Morgan performed the investigation. S.M.E. Smith and T.E. DeCoursey administered the project. S. Thomas and S.M.E. Smith provided the resources. S.M.E. Smith and T.E. DeCoursey visualized the study. T.E. DeCoursey wrote the original draft of the manuscript. S.M.E. Smith and T.E. DeCoursey reviewed and edited the manuscript.

Richard W. Aldrich served as editor.

Submitted: 7 December 2017
Accepted: 27 March 2018

References

Bennett, A.L., and I.S. Ramsey. 2017. CrossTalk opposing view: proton transfer in Hv1 utilizes a water wire, and does not require transient protonation of a conserved aspartate in the S1 transmembrane helix. *J. Physiol.* 595:6797–6799. https://doi.org/10.1113/JP274553

Berger, T.K., D.M. Fußhöller, N. Goodwin, W. Bönigk, A. Müller, N. Dokani Khesroshahi, C. Brenker, D. Wachten, E. Krause, U.B. Kaupp, and T. Strünker. 2017. Post-translational cleavage of Hv1 in human sperm tunes pH- and voltage-dependent gating. *J. Physiol.* 595:1533–1546. https://doi.org/10.1113/JP273189

Bernheim, L., R.M. Krause, A. Baroffio, M. Hamann, A. Kaelin, and C.R. Bader. 1993. A voltage-dependent proton current in cultured human skeletal muscle myotubes. *J. Physiol.* 470:313–333. https://doi.org/10.1113/jphysiol.1993.sp019860

Byerly, L., R. Meech, and W. Moody Jr. 1984. Rapidly activating hydrogen ion currents in perfused neurones of the snail, *Lymnaea stagnalis*. *J. Physiol.* 351:199–216. https://doi.org/10.1113/jphysiol.1984.sp015241

Chakraborty, A., S. Mandloi, C.J. Lanczycki, A.R. Panchenko, and S. Chakrabarti. 2012. SPEER-SERVER: a web server for prediction of protein specificity determining sites. *Nucleic Acids Res.* W242-W248. https://doi.org/10.1093/nar/gks559

Chamberlin, A., F. Qiu, S. Rebolledo, Y. Wang, S.Y. Noskov, and H.P. Larsson. 2014. Hydrophobic plug functions as a gate in voltage-gated proton channels. *Proc. Natl. Acad. Sci. USA.* 111:E273–E282. https://doi.org/10.1073/pnas.1318018111

Chaves, G., C. Derst, A. Franzen, Y. Mashimo, R. Machida, and B. Musset. 2016. Identification of an H_V 1 voltage-gated proton channel in insects. *FEBS J.* 283:1453–1464. https://doi.org/10.1111/febs.13680

Cherny, V.V., and T.E. DeCoursey. 1999. pH-dependent inhibition of voltage-gated H^+ currents in rat alveolar epithelial cells by Zn^{2+} and other divalent cations. *J. Gen. Physiol.* 114:819–838. https://doi.org/10.1085/jgp.114.6.819

Cherny, V.V., V.S. Markin, and T.E. DeCoursey. 1995. The voltage-activated hydrogen ion conductance in rat alveolar epithelial cells is determined by the pH gradient. *J. Gen. Physiol.* 105:861–896. https://doi.org/10.1085/jgp.105.6.861

Cherny, V.V., L.M. Henderson, and T.E. DeCoursey. 1997. Proton and chloride currents in Chinese hamster ovary cells. *Membr. Cell Biol.* 11:337–347.

Cherny, V.V., R. Murphy, V. Sokolov, R.A. Levis, and T.E. DeCoursey. 2003. Properties of single voltage-gated proton channels in human eosinophils estimated by noise analysis and by direct measurement. *J. Gen. Physiol.* 121:615–628. https://doi.org/10.1085/jgp.200308813

Cherny, V.V., D. Morgan, B. Musset, G. Chaves, S.M.E. Smith, and T.E. DeCoursey. 2015. Tryptophan 207 is crucial to the unique properties of the human voltage-gated proton channel, hH_V1. *J. Gen. Physiol.* 146:343–356. https://doi.org/10.1085/jgp.201511456

DeCoursey, T.E. 1991. Hydrogen ion currents in rat alveolar epithelial cells. *Biophys. J.* 60:1243–1253. https://doi.org/10.1016/S0006-3495(91)82158-0

DeCoursey, T.E. 2003. Voltage-gated proton channels and other proton transfer pathways. *Physiol. Rev.* 83:475–579. https://doi.org/10.1152/physrev.00028.2002

DeCoursey, T.E. 2010. Voltage-gated proton channels find their dream job managing the respiratory burst in phagocytes. *Physiology (Bethesda).* 25:27–40. https://doi.org/10.1152/physiol.00039.2009

DeCoursey, T.E. 2013. Voltage-gated proton channels: molecular biology, physiology, and pathophysiology of the H_V family. *Physiol. Rev.* 93:599–652. https://doi.org/10.1152/physrev.00011.2012

DeCoursey, T.E. 2015. The voltage-gated proton channel: a riddle, wrapped in a mystery, inside an enigma. *Biochemistry.* 54:3250–3268. https://doi.org/10.1021/acs.biochem.5b00353

DeCoursey, T.E. 2017. CrossTalk proposal: Proton permeation through H_V1 requires transient protonation of a conserved aspartate in the S1 transmembrane helix. *J. Physiol.* 595:6793–6795. https://doi.org/10.1113/JP274495

DeCoursey, T.E. 2018. Voltage and pH sensing by the voltage-gated proton channel, H_V1. *J. R. Soc. Interface.* 15:20180108. https://doi.org/10.1098/rsif.2018.0108

DeCoursey, T.E., and V.V. Cherny. 1993. Potential, pH, and arachidonate gate hydrogen ion currents in human neutrophils. *Biophys. J.* 65:1590–1598. https://doi.org/10.1016/S0006-3495(93)81198-6

DeCoursey, T.E., and V.V. Cherny. 1995. Voltage-activated proton currents in membrane patches of rat alveolar epithelial cells. *J. Physiol.* 489:299–307. https://doi.org/10.1113/jphysiol.1995.sp021051

DeCoursey, T.E., and V.V. Cherny. 1997. Deuterium isotope effects on permeation and gating of proton channels in rat alveolar epithelium. *J. Gen. Physiol.* 109:415–434. https://doi.org/10.1085/jgp.109.4.415

DeCoursey, T.E., and V.V. Cherny. 1998. Temperature dependence of voltage-gated H^+ currents in human neutrophils, rat alveolar epithelial cells, and mammalian phagocytes. *J. Gen. Physiol.* 112:503–522. https://doi.org/10.1085/jgp.112.4.503

DeCoursey, T.E., D. Morgan, and V.V. Cherny. 2003. The voltage dependence of NADPH oxidase reveals why phagocytes need proton channels. *Nature.* 422:531–534. https://doi.org/10.1038/nature01523

DeCoursey, T.E., D. Morgan, B. Musset, and V.V. Cherny. 2016. Insights into the structure and function of H_V1 from a meta-analysis of mutation studies. *J. Gen. Physiol.* 148:97–118. https://doi.org/10.1085/jgp.201611619

Demaurex, N., S. Grinstein, M. Jaconi, W. Schlegel, D.P. Lew, and K.H. Krause. 1993. Proton currents in human granulocytes: regulation by membrane potential and intracellular pH. *J. Physiol.* 466:329–344.

Dudev, T., B. Musset, D. Morgan, V.V. Cherny, S.M.E. Smith, K. Mazmanian, T.E. DeCoursey, and C. Lim. 2015. Selectivity mechanism of the voltage-gated proton channel, H_V1. *Sci. Rep.* 5:10320. https://doi.org/10.1038/srep10320

Gordienko, D.V., M. Tare, S. Parveen, C.J. Fenech, C. Robinson, and T.B. Bolton. 1996. Voltage-activated proton current in eosinophils from human blood. *J. Physiol.* 496:299–316. https://doi.org/10.1113/jphysiol.1996.sp021686

Gu, X., and H. Sackin. 1995. Effect of pH on potassium and proton conductance in renal proximal tubule. *Am. J. Physiol.* 269:F289–F308. https://doi.org/10.1152/ajprenal.1995.269.3.F289

Henderson, L.M., J.B. Chappell, and O.T.G. Jones. 1987. The superoxide-generating NADPH oxidase of human neutrophils is electrogenic and associated with an H^+ channel. *Biochem. J.* 246:325–329. https://doi.org/10.1042/bj2460325

Kapus, A., R. Romanek, A.Y. Qu, O.D. Rotstein, and S. Grinstein. 1993. A pH-sensitive and voltage-dependent proton conductance in the plasma membrane of macrophages. *J. Gen. Physiol.* 102:729–760. https://doi.org/10.1085/jgp.102.4.729

Katoh, K., and D.M. Standley. 2013. MAFFT multiple sequence alignment software version 7: improvements in performance and usability. *Mol. Biol. Evol.* 30:772–780. https://doi.org/10.1093/molbev/mst010

Koch, H.P., T. Kurokawa, Y. Okochi, M. Sasaki, Y. Okamura, and H.P. Larsson. 2008. Multimeric nature of voltage-gated proton channels. *Proc. Natl. Acad. Sci. USA.* 105:9111–9116. https://doi.org/10.1073/pnas.0801553105

Kulleperuma, K., S.M.E. Smith, D. Morgan, B. Musset, J. Holyoake, N. Chakrabarti, V.V. Cherny, T.E. DeCoursey, and R. Pomès. 2013. Construction and validation of a homology model of the human voltage-gated proton channel hH_V1. *J. Gen. Physiol.* 141:445–465. https://doi.org/10.1085/jgp.201210856

Kuno, M., H. Ando, H. Morihata, H. Sakai, H. Mori, M. Sawada, and S. Oiki. 2009. Temperature dependence of proton permeation through a voltage-gated proton channel. *J. Gen. Physiol.* 134:191–205. https://doi.org/10.1085/jgp.200910213

Lee, S.Y., J.A. Letts, and R. Mackinnon. 2008. Dimeric subunit stoichiometry of the human voltage-dependent proton channel Hv1. *Proc. Natl. Acad. Sci. USA.* 105:7692–7695. https://doi.org/10.1073/pnas.0803277105

Li, Q., R. Shen, J.S. Treger, S.S. Wanderling, W. Milewski, K. Siwowska, F. Bezanilla, and E. Perozo. 2015. Resting state of the human proton channel dimer in a lipid bilayer. *Proc. Natl. Acad. Sci. USA.* 112:E5926–E5935. https://doi.org/10.1073/pnas.1515043112

Morgan, D., B. Musset, K. Kulleperuma, S.M.E. Smith, S. Rajan, V.V. Cherny, R. Pomès, and T.E. DeCoursey. 2013. Peregrination of the selectivity filter delineates the pore of the human voltage-gated proton channel hH_V1. *J. Gen. Physiol.* 142:625–640. https://doi.org/10.1085/jgp.201311045

Murphy, R., and T.E. DeCoursey. 2006. Charge compensation during the phagocyte respiratory burst. *Biochim. Biophys. Acta.* 1757:996–1011. https://doi.org/10.1016/j.bbabio.2006.01.005

Musset, B., V.V. Cherny, D. Morgan, Y. Okamura, I.S. Ramsey, D.E. Clapham, and T.E. DeCoursey. 2008. Detailed comparison of expressed and native voltage-gated proton channel currents. *J. Physiol.* 586:2477–2486. https://doi.org/10.1113/jphysiol.2007.149427

Musset, B., S.M.E. Smith, S. Rajan, V.V. Cherny, S. Sujai, D. Morgan, and T.E. DeCoursey. 2010. Zinc inhibition of monomeric and dimeric proton channels suggests cooperative gating. *J. Physiol.* 588:1435–1449. https://doi.org/10.1113/jphysiol.2010.188318

Musset, B., S.M.E. Smith, S. Rajan, D. Morgan, V.V. Cherny, and T.E. DeCoursey. 2011. Aspartate112 is the selectivity filter of the human voltage-gated proton channel. *Nature.* 480:273–277. https://doi.org/10.1038/nature10557

Nordström, T., O.D. Rotstein, R. Romanek, S. Asotra, J.N. Heersche, M.F. Manolson, G.F. Brisseau, and S. Grinstein. 1995. Regulation of cytoplasmic pH in osteoclasts. Contribution of proton pumps and a proton-selective conductance. *J. Biol. Chem.* 270:2203–2212. https://doi.org/10.1074/jbc.270.5.2203

Ramsey, I.S., Y. Mokrab, I. Carvacho, Z.A. Sands, M.S.P. Sansom, and D.E. Clapham. 2010. An aqueous H$^+$ permeation pathway in the voltage-gated proton channel Hv1. *Nat. Struct. Mol. Biol.* 17:869–875. https://doi.org/10.1038/nsmb.1826

Rodriguez, J.D., S. Haq, T. Bachvaroff, K.F. Nowak, S.J. Nowak, D. Morgan, V.V. Cherny, M.M. Sapp, S. Bernstein, A. Bolt, et al. 2017. Identification of a vacuolar proton channel that triggers the bioluminescent flash in dinoflagellates. *PLoS One.* 12:e0171594. https://doi.org/10.1371/journal.pone.0171594

Sakata, S., N. Miyawaki, T.J. McCormack, H. Arima, A. Kawanabe, N. Özkucur, T. Kurokawa, Y. Jinno, Y. Fujiwara, and Y. Okamura. 2016. Comparison between mouse and sea urchin orthologs of voltage-gated proton channel suggests role of S3 segment in activation gating. *Biochim. Biophys. Acta.* 1858:2972–2983. https://doi.org/10.1016/j.bbamem.2016.09.008

Schilling, T., A. Gratopp, T.E. DeCoursey, and C. Eder. 2002. Voltage-activated proton currents in human lymphocytes. *J. Physiol.* 545:93–105. https://doi.org/10.1113/jphysiol.2002.028878

Schrenzel, J., D.P. Lew, and K.H. Krause. 1996. Proton currents in human eosinophils. *Am. J. Physiol.* 271:C1861–C1871. https://doi.org/10.1152/ajpcell.1996.271.6.C1861

Smith, S.M.E., D. Morgan, B. Musset, V.V. Cherny, A.R. Place, J.W. Hastings, and T.E. DeCoursey. 2011. Voltage-gated proton channel in a dinoflagellate. *Proc. Natl. Acad. Sci. USA.* 108:18162–18167. https://doi.org/10.1073/pnas.1115405108

Szteyn, K., W. Yang, E. Schmid, F. Lang, and E. Shumilina. 2012. Lipopolysaccharide-sensitive H$^+$ current in dendritic cells. *Am. J. Physiol. Cell Physiol.* 303:C204–C212. https://doi.org/10.1152/ajpcell.00059.2012

Takeshita, K., S. Sakata, E. Yamashita, Y. Fujiwara, A. Kawanabe, T. Kurokawa, Y. Okochi, M. Matsuda, H. Narita, Y. Okamura, and A. Nakagawa. 2014. X-ray crystal structure of voltage-gated proton channel. *Nat. Struct. Mol. Biol.* 21:352–357. https://doi.org/10.1038/nsmb.2783

Thomas, S., V.V. Cherny, D. Morgan, L.R. Artinian, V. Rehder, S.M.E. Smith, and T.E. DeCoursey. 2018. Exotic properties of a voltage-gated proton channel from the snail *Helisoma trivolvis. J. Gen. Physiol.* https://doi.org/10.1085/201711967

Tombola, F., M.H. Ulbrich, and E.Y. Isacoff. 2008. The voltage-gated proton channel Hv1 has two pores, each controlled by one voltage sensor. *Neuron.* 58:546–556. https://doi.org/10.1016/j.neuron.2008.03.026

van Keulen, S.C., E. Gianti, V. Carnevale, M.L. Klein, U. Rothlisberger, and L. Delemotte. 2017. Does proton conduction in the voltage-gated H$^+$ channel hHv1 involve Grotthuss-like hopping via acidic residues? *J. Phys. Chem. B.* 121:3340–3351. https://doi.org/10.1021/acs.jpcb.6b08339

Walther, D., and P. Argos. 1996. Intrahelical side chain-side chain contacts: the consequences of restricted rotameric states and implications for helix engineering and design. *Protein Eng.* 9:471–478. https://doi.org/10.1093/protein/9.6.471